Reconfigurable optical quadrature amplitude modulation converter/encoder using a tunable complex coefficient optical tapped delay line

Salman Khaleghi,[1,*] Mohammad Reza Chitgarha,[1] Omer F. Yilmaz,[1] Moshe Tur,[2] Michael W. Haney,[3] Carsten Langrock,[4] Martin M. Fejer,[4] and Alan E. Willner[1]

[1]*Department of Electrical Engineering, University of Southern California, Los Angeles, California 90089, USA*

[2]*School of Electrical Engineering, Tel Aviv University, Ramat Aviv 69978, Israel*

[3]*Department of Electrical and Computer Engineering, University of Delaware, Newark, Delaware 19716, USA*

[4]*Edward L. Ginzton Laboratory, Stanford University, Stanford, California 94305, USA*

**Corresponding author: khaleghi@usc.edu*

Received March 5, 2013; accepted March 27, 2013;
posted April 8, 2013 (Doc. ID 186426); published May 3, 2013

We experimentally demonstrate a reconfigurable optical converter/encoder for quadrature amplitude modulated (QAM) signals. The system utilizes nonlinear wavelength multicasting, conversion-dispersion delays, and simultaneous nonlinear multiplexing and sampling. We show baud rate tunability (31 and 20 Gbaud) and reconfigurable conversions from lower-order QAM signals to higher-order QAM signals (e.g., 64-QAM). © 2013 Optical Society of America

OCIS codes: (060.2360) Fiber optics links and subsystems; (060.4370) Nonlinear optics, fibers; (190.4223) Nonlinear wave mixing.

http://dx.doi.org/10.1364/OL.38.001600

The increasing demand for higher capacity in optical networks has made it a challenge to efficiently use the available bandwidth. Owing to the recent advances in the fields of high-speed digital signal processing and analog-to-digital converters (ADCs), use of spectrally efficient quadrature amplitude modulation (QAM) formats together with optical coherent receivers has gained interest as a possible solution. In transparent optical networks, where various modulation formats and different baud rates are used, a laudable goal might be to encode and convert a signal from a simpler modulation format, such as binary phase shift keying (BPSK) or quadrate phase shift keying (QPSK), to a higher-order QAM format, such as 16-QAM or 64-QAM [1,2]. Besides the potential for increasing the spectral efficiency, conversion/encoding of QAM symbols is quite valuable for many types of coding, including encryption/decryption and error correction [3]. To accommodate various modulation schemes, such system should probably be bit-rate and data-format transparent [4].

Reports on QAM signal generation and conversion span both electronic and all-optical approaches [2]. All-optical techniques hold the promise for QAM generation at high baud rates without the strict linearity and bandwidth constraints of electronic amplifiers. Previously published results on the optical techniques include: (a) electro-optic digital-to-analog conversion using parallel modulators [5], (b) multiplexing of two 10 Gbaud QPSK signals to star 16-QAM [1], and (c) simulations on various QAM generation using dual-parallel Mach–Zehnder modulator (MZM) and phase modulators [6]. Most of these techniques are generally limited to certain modulation formats, and some require multiple separate input channels. Given the importance of QAM signals, a desirable goal would be to achieve an optical QAM encoder/converter that can accommodate various input/output modulation formats and operate on a single channel to increase its spectral efficiency.

In this Letter, we experimentally demonstrate a reconfigurable and fully tunable QAM encoder/converter that utilizes a nonlinear sampler incorporated in a coherent complex coefficient optical tunable tapped delay line [4] to simultaneously convert and sample 20 and 31 Gbaud BSPK/QPSK signals to 4/8/16/64-QAM [7].

Figure 1 depicts the conceptual block diagram of the QAM converter/encoder using an example for QPSK to 64-QAM conversion. In principle, if consecutive lower-order and higher baud rate input QAM symbols (e.g., BPSK or QPSK) are coherently combined and sampled, they can generate a higher-order and lower baud rate output QAM signal. If $x(t)$ is the input signal, the output signal, $y(t)$ is:

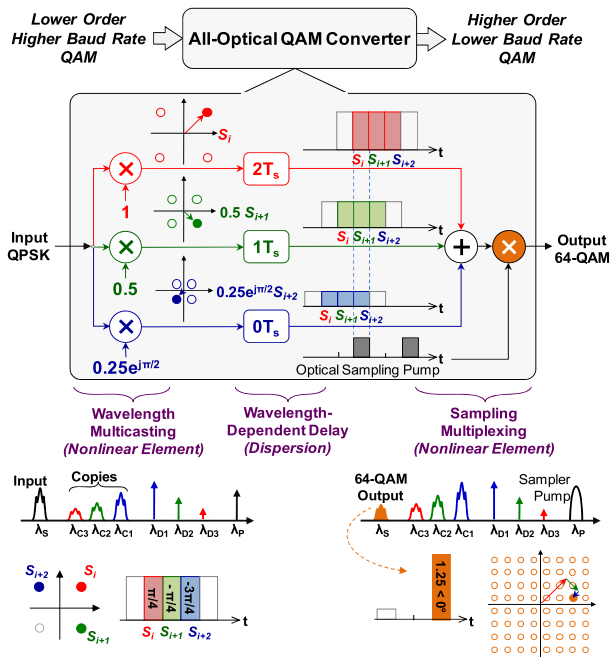

Fig. 1. Conceptual block diagram of an optical QAM format converter using nonlinear signal processing.

$$y(t) \propto \sum_{i=0}^{\infty} \Pi(t - iNT_s) \times \sum_{i=1}^{N} c_i x(t - (i-1)T_s) \quad (1)$$

in which, $\Pi(t)$ is a pulse function which has unit amplitude from time 0 to T_s (symbol time) and is zero outside this range. The second summation represents a tapped delay line with N taps and complex tap coefficients c_i [4]. The first summation is in fact a pulse train that samples the output of the tapped delay line every N symbol. In the case of QPSK to 64-QAM conversion, N is 3 and coefficients (c_i) can be [1, 0.5, 0.25j]. After sampling, the available free time slots can be used for time division multiplexing. If sampling is not used, the output would be a 64-QAM signal at the baud rate of the original QPSK signal, which now carries two redundant symbols for every three symbols. This symbol redundancy could be used in coded modulation formats in conjunction with Viterbi algorithm (with only 4 states) [3]. Sampling can eliminate this redundancy. We demonstrate a system that not only can encode/convert arbitrary constellation points using basic weighting, vector rotation, and addition functionalities, but can also simultaneously sample the resulting signal. The signal is first copied to multiple wavelengths in a nonlinear device in a process known as multicasting. The signal copies are then sent into a dispersive element in which different wavelengths travel at different speeds. The signals are then coherently multiplexed and sampled in another nonlinear device to create the output [7].

Figure 2 depicts the experimental setup. The input BPSK/QPSK signal is generated by driving an IQ modulator with pseudorandom bit sequence (PRBS) $2^{31} - 1$ to modulate a continuous wave (CW) laser at wavelength λ_S (angular frequency ω_S). The signal is then combined with four amplified CW dummy pump lasers (λ_{D1} to λ_{D4}) and another amplified CW pump at λ_P and is sent into a nonlinear periodically poled lithium niobate (PPLN) waveguide. The signal λ_S and the pump λ_P are located symmetrically with respect to the quasi-phase matching frequency (QPM) of the waveguide; therefore, they can mix through the $\chi^{(2)}$ sum frequency generation (SFG) process. The SFG signal then mixes with multiple λ_{Di} pumps through difference frequency generation (DFG)

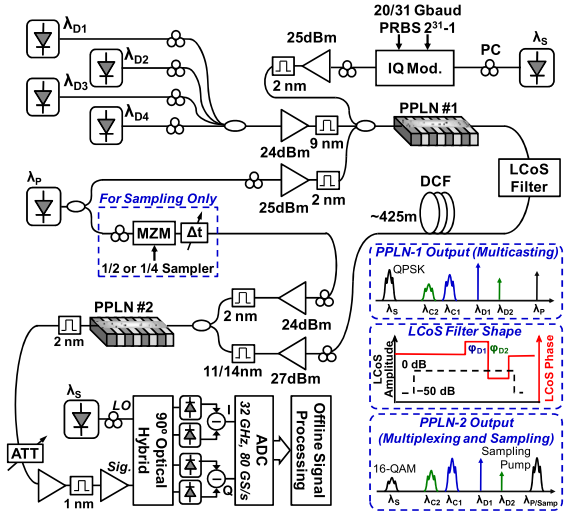

Fig. 2. Experimental setup and schematic wave-mixing spectra. PC, polarization controller; ATT, attenuator; LO, local oscillator.

process and produces multiple replicas of the input data signal [4]. The center frequency of the generated signal copies ($\omega_{Ci} = \omega_S + \omega_P - \omega_{Di}$) and their complex amplitude ($A_{Ci}(t) \propto A_S(t) A_P A_{Di}^*$) are determined by the conservation of energy and phase-matching rules, respectively, [the asterisk $(\cdot)^*$ denotes the complex conjugate] [8]. The output is then sent into a phase/amplitude programmable liquid crystal on silicon (LCoS) filter that (i) blocks the original data signal and the λ_P pump, and (ii) applies phase shift of ϕ_i on the λ_{Di} pumps (Fig. 2, schematic spectra). Keeping the original dummy pumps and their corresponding signal copies on the same path will maintain the phase coherency required for coherent addition in the final stage. Subsequently, the signal copies and the dummy pumps are sent through a dispersion compensating fiber (DCF). In the DCF, each signal copy travels at a different speed, resulting in a relative time delay of $\Delta T = DL\Delta\lambda$ between the signals (D is the fiber dispersion, L is the DCF length, and $\Delta\lambda$ is the wavelength separation of two signal copies). $\Delta\lambda$ is chosen such that the adjacent signal copies are delayed by one symbol time (T_s) after the DCF. Next, the delayed signals and pumps are combined with a sampling pump ($\lambda_{P/\mathrm{Samp}}$) and sent into the second PPLN waveguide, where similar cascaded SFG and DFG wave mixings produce a multiplexed signal at frequency $\omega_{\mathrm{MUX}} = \omega_{Di} + \omega_{Ci} - \omega_{P/\mathrm{Samp}} = \omega_S + (\omega_P - \omega_{P/\mathrm{Samp}})$ with complex amplitude proportional to $(A_{Di} e^{j\phi_i}) A_{Ci}(t - (i-1)T_s) A_{P/\mathrm{Samp}}^*(t)$. Therefore, the total resulting multiplexed and sampled output is

$$A_{\mathrm{MUX}}(t) \propto A_{P/\mathrm{Samp}}^*(t) \sum_{i=1}^{N} |A_{Di}|^2 e^{j\phi_i} A_S(t - (i-1)T_s). \quad (2)$$

Equation (2) replicates Eq. (1) and is the mathematical representation of the optical QAM encoder/converter. The converter/encoder can be reconfigured by varying the properties of the pump lasers fed into the system: N (number of dummy pump lasers), $|c_i|$ (λ_{Di} laser power), $\measuredangle c_i$ (LCoS phase on λ_{Di}), T_s (spacing between λ_{Di}'s). For example, 3 dB attenuation on a dummy pump power translates to a factor of 0.5 in the coefficient. The sampling rate should be set to $1/N$.

As shown in Fig. 2, 20 and 31 Gbaud rates are chosen (31 GHz is chosen for better electronic signal quality). The DCF length is $L \approx 425$ m with $D \approx -80$ s/nm/km dispersion. Therefore, if the adjacent dummy pumps are located $\Delta\lambda = 0.95$ m apart, the induced delay is one 31 Gbaud symbol time $T_s = DL\Delta\lambda \approx 32.25$ ps. For 20 Gbaud signals, the pump spacing is increased to 1.46 nm. The first and the second PPLN waveguides are 4 and 5 cm long, respectively, and their QPM wavelengths are thermally tuned to ~1549.6 nm. The signal wavelength λ_S is ~1540.9 nm and the λ_P pump is ~1558.3 nm. For experiments with a sampling pump, $\lambda_{P/\mathrm{Samp}}$ pump is generated by driving a MZM with a pulse train at half-clock or quarter-clock repetition rate, followed by an optical tunable delay line for synchronization. The output signal is filtered, sent into a preamplified receiver and coherently detected using a local oscillator at wavelength ~λ_S, an optical hybrid, balanced photodiodes, and 32 GHz bandwidth 80 GSample/s ADC. Offline signal processing is used to recover the constellation diagrams.

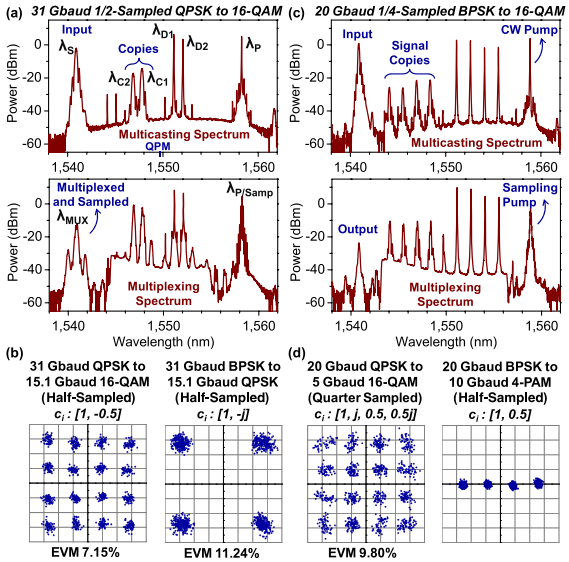

Fig. 3. (a) Spectra of the first and the second PLLN waveguides outputs for 31 Gbaud input signal with half-rate sampling pump. (b) Output constellations. (c) Spectra for 20 Gbaud signals, and (d) output constellations.

Figure 3(a) depicts the output spectra of the multicasting and multiplexing stages for conversion of 31 Gbaud QPSK to 15.5 Gbaud 16-QAM using a half-rate sampling pump in the second stage. λ_{D2} has 3 dB lower power than λ_{D1} and 180° phase shift is applied on it in the LCoS filter, resulting in coefficients of $c_i = [1, -0.5]$. The constellation diagram is shown in Fig. 3(b) together with results of another configuration where the input is BPSK and the coefficients are set to $c_i = [1, j]$ to create QPSK output. The error vector magnitudes (EVMs) are also noted in Fig. 3. Figures 3(c) and 3(d) show results on 20 Gbaud signals with quarter sampling (5 GHz repetition rate) for generation of a 16-QAM symbol from four BPSK symbols, demonstrating reconfigurability for different baud rates and encodings. The coefficients determine the encoding of the generated 16-QAM. The 20 Gbaud system is reconfigured by turning off two lasers to create a 4-PAM signal, as shown in Fig. 3(d).

In Fig. 4, a CW pump is used instead of the sampling pulse, resulting in generation of signals with higher-order QAM and same baud rate. Figure 4(a) depicts the spectra for generation of 31 Gbaud 64-QAM signal by combining

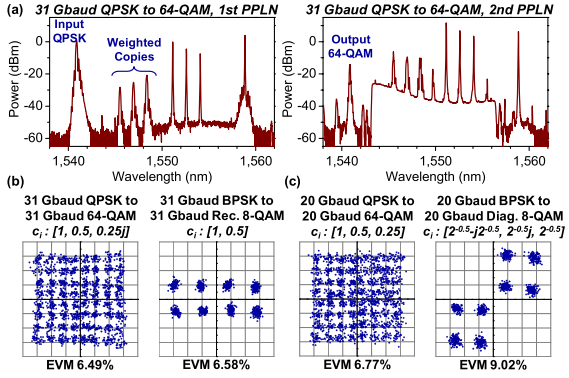

Fig. 4. (a) Output spectra of nonlinear stages for QPSK to 64-QAM conversion. Constellation diagrams showing different encodings for (b) 31 Gbaud and (c) 20 Gbaud signals.

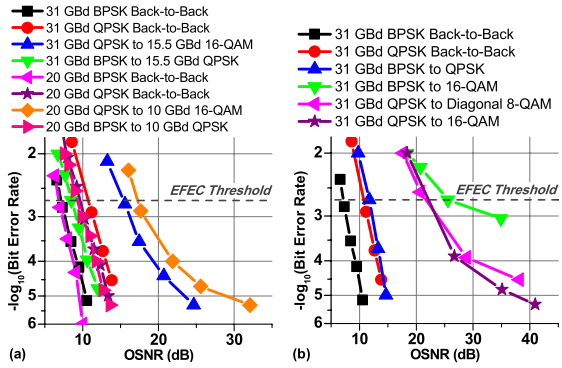

Fig. 5. BER measurements versus OSNR for experiments with (a) a sampling pump and (b) with a CW pump.

three QPSK symbols using coefficients $c_i = [1, 0.5, 0.25]$. The 64-QAM constellations for 31 and 20 Gbaud are shown in Figs. 4(b) and 4(c). The constellation diagrams for two sample arbitrary 8-QAM formats are also depicted showing other phase and amplitude reconfigurations.

Bit error rate (BER) measurements versus optical signal-to-noise ratio (OSNR) are shown in Fig. 5. For sampling pump experiments, the measured OSNR penalty at BER $= 2 \times 10^{-3}$ is ~2 dB and ~5 dB for conversions of 31 Gbaud BPSK to 15.5 Gbaud QPSK and 31 Gbaud QPSK to 15.5 Gbaud 16-QAM, respectively. Due to the transmitter's higher signal distortion for 20 Gbaud QPSK, the BER results are slightly better at 31 Gbaud. In nonsampling experiments, the OSNR penalty for generation of QPSK from BPSK is ~1 dB compared to back-to-back measured QPSK. 16-QAM obtained from QPSK, and 16-QAM generated from BPSK, required ~3 dB and ~7 dB higher OSNR compared to a back-to-back 10 Gbaud 16-QAM, respectively, (10 Gbaud 16-QAM requires ~19 dB OSNR for BER of 2×10^{-3}).

We acknowledge the support of DARPA under the contracts FA8650-08-1-7820, HR0011-11-1-0015, and W911NF-10-1-0151 and NSF CIAN (contract 0812072).

References

1. L. Yan, A. E. Willner, X. Wu, A. Yi, A. Bogoni, Z.-Y. Chen, and H.-Y. Jiang, J. Lightwave Technol. **30**, 3760 (2012).
2. A. H. Gnauck, P. J. Winzer, A. Konczykowska, F. Jorge, J.-Y. Dupuy, M. Riet, G. Charlet, B. Zhu, and D. W. Peckham, J. Lightwave Technol. **30**, 532 (2012).
3. J. G. Proakis, *Digital Communications* (McGraw-Hill, 2000).
4. S. Khaleghi, O. F. Yilmaz, M. R. Chitgarha, M. Tur, N. Ahmed, S. R. Nuccio, I. M. Fazal, X. Wu, M. W. Haney, C. Langrock, M. M. Fejer, and A. E. Willner, IEEE Photon. J. **4**, 511, (1995).
5. T. Sakamoto and A. Chiba, IEEE J. Sel. Top. Quantum Electron. **16**, 1140 (2010).
6. L. Zhang, X. Hu, Y. Wu, Q. Liu, T. Wang, and Y. Su, in *15th Asia-Pacific Conference on Communications* (IEEE, 2009), 609.
7. S. Khaleghi, M. R. Chitgarha, O. F. Yilmaz, H. Huang, M. Tur, M. W. Haney, and A. E. Willner, in *Proceedings of the IEEE/OSA Conference on Optical Fiber Communications* (IEEE, 2012), paper OTh4H.6.
8. C. Langrock, S. Kumar, J. E. McGeehan, A. E. Willner, and M. M. Fejer, J. Lightwave Technol. **24**, 2579 (2006).